Human Movement Science 88 (2023) 103054

Contents lists available at ScienceDirect

Human Movement Science

journal homepage: www.elsevier.com/locate/humov

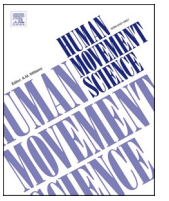

Reference values and functional descriptions of transverse plane spinal dynamics during gait based on surface topography

Janine Huthwelker [a], Jürgen Konradi [a], Claudia Wolf [a], Ruben Westphal [b], Irene Schmidtmann [b], Patric Schubert [c], Philipp Drees [d], Ulrich Betz [a,*]

[a] Institute of Physical Therapy, Prevention and Rehabilitation, University Medical Center of the Johannes Gutenberg University Mainz, Langenbeckstrasse 1, D-55131 Mainz, Germany
[b] Institute of Medical Biostatistics, Epidemiology and Informatics, University Medical Center of the Johannes Gutenberg University Mainz, Obere Zahlbacher Straße 69, D-55131 Mainz, Germany
[c] Institute of Complex Health Sciences, Hochschule Fresenius, University of Applied Sciences, Limburgerstr. 2, D-65510 Idstein, Germany
[d] Department of Orthopedics and Trauma Surgery, University Medical Center of the Johannes Gutenberg University Mainz, Langenbeckstrasse 1, D-55131 Mainz, Germany

ARTICLE INFO

Keywords:
Videorasterstereography
Gait analysis
Motion analysis
Normative values
Healthy human spine

ABSTRACT

Spinal dynamics during gait have been of interest in research for many decades. Based on respective previous investigations, the pelvis is generally expected to be maximally forward rotated on the side of the reference leg at the beginning of each gait cycle and to reach its maximum counterrotation approximately at the end of the reference leg's stance phase. The pelvic–upper-thoracic-spine coordination converges towards an anti-phase movement pattern in high velocities during ambulation. The vertebral bodies around the seventh thoracic vertebra are considered to be an area of transition during human ambulation where no or at least little rotary motion can be observed. The respective cranial and caudal vertebrae meanwhile are expected to rotate conversely around this spinal point of intersection. However, these previous assumptions are based on scarce existing research, whereby only isolated vertebrae have been analyzed contemporaneously. Due to huge methodological differences in data capturing approaches, the results are additionally hardly comparable to each other and involved measurement procedures are often not implementable in clinical routines. Furthermore, none of the above-mentioned methods provided reference data for spinal motion during gait based on an appropriate number of healthy participants. Hence, the aim of this study was to present such reference data for spinal rotary motion of every vertebral body from C7 down to L4 and the pelvis derived from surface topographic back shape analyses in a cohort of 201 healthy participants walking on a treadmill at a given walking speed of 5 km/h. Additionally, the spine's functional movement behavior during gait should be described in the transverse plane based on data derived from this noninvasive, clinically suitable measurement approach and, in conclusion, the results shall be compared against those of previous research findings derived from other measurement techniques. Contrary to the previous functional understanding, the area of the mid-thoracic spine was found to demonstrate the largest amplitude of rotary motion of all investigated vertebrae and revealed an approximately counterrotated movement behavior compared to the rotary motion of the pelvis. In both directions, spinal rotation during gait seemed to be initiated by the pelvis. The overlying vertebrae followed in succession in the sense of an ongoing movement. Therefore, the

* Corresponding author.
E-mail address: Ulrich.Betz@unimedizin-mainz.de (U. Betz).

https://doi.org/10.1016/j.humov.2022.103054
Received 10 June 2022; Received in revised form 30 November 2022; Accepted 26 December 2022
Available online 6 January 2023

point of intersection was not statically located in a specific anatomical section of the spine. Instead, it was found to be dynamic, ascending from one vertebra to the next from caudal to cranial in dependence of the pelvis's rotation initiation.

1. Introduction

Back pain is still a health problem of outstanding medical, epidemiological and economical importance (Raspe, 2012) and asymmetrical, respectively irregular movement patterns or changes in the pelvic–thorax coordination during gait are associated with low-back pain disorders (Kakushima, Miyamoto, & Shimizu, 2003; Lamoth et al., 2002; Vogt, Pfeifer, Portscher, & Banzer, 2001). However, even for the healthy population there is no proper understanding of the precise motion pattern of each individual vertebral body during gait. So far, the literature only provides a rough functional framework whose details remain unclear. The pelvis is generally expected to reach its maximally forward rotated position on the side of the reference leg at the beginning of each gait cycle (initial contact) and to reach its maximum counterrotation at the end of the reference leg's stance phase (terminal stance) (Perry & Burnfield, 2010). The pelvis–thorax coordination (measured between the pelvis and the anatomical height of the shoulders) evolves from an in-phase towards an almost anti-phase movement pattern with increasing velocity during ambulation (1.4 km/h – 5.4 km/h) (Lamoth, Beek, & Meijer, 2002). Additionally, an early invasive measurement approach, using Steinmann pins and a relative-rotation transducer, found the seventh thoracic vertebra to be an area of transition during human ambulation, where no, or at least little, rotary motion can be observed (Gregersen & Lucas, 1967). The pelvis and the lumbar spine were described to be forwardly rotated at heel strike in terms of a functional unit. Further up, the rotation of the lower thoracic spine diminishes gradually until zero degrees at the seventh thoracic vertebra. The counterrotation of the upper-thoracic spine gradually increased from the seventh thoracic vertebra upwards and reached its maximum at the first thoracic vertebra. Needham et al. (Needham, Naemi, Healy, & Chockalingam, 2016) investigated three isolated vertebrae using an optoelectronic motion capturing device (T3, T8 and L3) and also found the mid-thoracic vertebra to be the one with the least rotational movement. These findings correspond with commonly used and widely accepted visual observation criteria in clinical gait analysis: In functional kinetics, for example, the "hypothetical standard" for human gait also expects the "frontotransverse diameter of the thorax" (~T7) to be dynamically stabilized rectangular to the direction of movement (Suppé, 2014; Suppé & Bongarz, 2013). Those findings support the assumption that in healthy individuals the vertebrae below the mid-thoracic spine (~T7) are expected to gradually increase their rotation downwards until the maximum rotation of the pelvis is achieved. In contrast, the vertebrae above ~T7 are expected to gradually increase their rotation in the opposite direction to enable and facilitate the typical counterrotation of the shoulder-girdle during gait.

Challenging results of this presumption came from Bruijn, Meijer, van Dieen, Kingma, and Lamoth (2008), who analyzed transverse plane pelvis and thorax rotations in relation to movements of the upper leg. Among others, they measured three-dimensional trunk movements by a 3D-cluster of infrared LEDs at the anatomic level of T6. Thereby the authors revealed that with increasing walking speed (2.0 km/h – 5.2 km/h), the pelvis–thorax coordination shifted from in-phase to out of phase with increasing gait velocity. As T6 represented thorax rotations, these findings provided initial indications that the vertebral bodies of the mid-thoracic spine might possibly not be the described area of transition during human gait where no or at least only little rotary motion occurs.

Nevertheless, based on huge methodological differences the results of previous research are hardly comparable to each other and, to the authors' knowledge, there are currently no reference data addressing the three-dimensional movement behavior of every single vertebra of the healthy human spine during gait in relation to a standardized gait cycle (SGC) available. So far, either only isolated/multiple spinal vertebrae have been marked and analyzed (Ceccato, de Seze, Azevedo, & Cazalets, 2009; D'Amico, D'Amico, Paniccia, Roncoletta, & Vallasciani, 2010; D'Amico, Kinel, D'Amico, & Roncoletta, 2021; Konz et al., 2006; Needham, Naemi, et al., 2016) or the vertebral column has been subdivided into large anatomic sections, respectively encompassing several vertebrae ("lumbar spine," "thorax," "trunk," etc.), which were regarded as almost rigid bodies in themselves and whose three-dimensional movement behavior during gait had then been described in multiple planes (Crosbie, Vachalathiti, & Smith, 1997; Feipel, De Mesmaeker, Klein, & Rooze, 2001; MacWilliams et al., 2013; Needham, Stebbins, & Chockalingam, 2016; Perry & Burnfield, 2010).

Additionally, invasive and noninvasive measurement approaches have to be distinguished from each other. MacWilliams et al. (2013) analyzed three-dimensional spinal movements during gait by inserting bone pins into the spinal process of each lumbar vertebra and attaching reflective markers laterally on the protruding pins. This procedure can theoretically be considered as a gold standard for motion analysis of spinal bony structures (Needham, Stebbins, & Chockalingam, 2016). However, by reasons of the surgical intervention and the required radiation exposure to control for the correct position of the pins, this approach is, just like the invasive procedure from Gregersen and Lucas (1967), inappropriate for use as a routine assessment in clinical as well as in scientific practice. Furthermore, the results have to be interpreted with caution because the participants' movement behavior might have been influenced by pain- or fear-induced inhibition of habitual movement patterns due to the surgical interventions.

In contrast, noninvasive reflective marker-based systems attached on the skin's surface, which are generally accepted to be the gold standard for three-dimensional analyses of human movements in clinical as well as in scientific practice (Needham, Stebbins, & Chockalingam, 2016), contain several limitations that have specifically been described for applications in the field of spinal motion analysis, and thereby particularly for data capturing in the transverse plane. These limitations include that for data capturing in the transverse plane each single vertebra of interest needs to be marked with three noncollinear markers (or a 3D cluster), respectively (Konz et al., 2006; Needham, Stebbins, & Chockalingam, 2016). Due to the small anatomic size of functional spinal units and the large number of required markers/3D-clusters to analyze every single vertebral body, the usability of marker-based technologies is limited

(Konz et al., 2006). Additionally, a large number of anatomic landmarks that have to be palpated and marked raise further difficulties (Chockalingam, Dangerfield, Giakas, & Cochrane, 2002) and the use of numerous 3D-clusters, even though they are from lightweight materials, is vulnerable to perturbations from impact forces created during walking (Needham, Stebbins, & Chockalingam, 2016). Such perturbations might possibly add up with other described and known effects of soft-tissue artifacts derived from marker-based motion analysis systems (Leardini, Chiari, Della Croce, & Cappozzo, 2005).

The ability, however, to further investigate spinal motion during gait by use of a suitable measurement tool able to capture three-dimensional motion of all vertebral bodies contemporaneously without usage of multiple markers, extensive preparation or the need for invasive or radiation-based measurement approaches would be of great value for the transferability of results into clinical practice as well as for future research. It could gain further knowledge of the healthy spine's functional movement behavior during gait and of the effects that different pathologies might possibly have on those movement patterns.

Surface topography (ST) might be just such a noninvasive and radiation-free alternative. It is based upon a stereophotogrammetric surface measurement approach, considers the Turner–Smith model (Turner-Smith, 1988; Turner-Smith, Harris, Houghton, & Jefferson, 1988), as well as the models of Drerup and Hierholzer (Drerup, 1993; Hierholzer, 1993) to not only analyze the participants' back surface, but also to precisely estimate every underlying vertebral body's position (C7–L4) and the pelvis in a virtually constructed three-dimensional model of the human spine (Drerup, Ellger, Meyer Zu Bentrup, & Hierholzer, 2001; Drerup & Hierholzer, 1994). During the last decades, ST was only applicable for static assessments of spinal posture and was predominantly used for the monitoring of progression in adolescent idiopathic scoliosis (Liljenqvist, Halm, Hierholzer, Drerup, & Weiland, 1998; Schulte et al., 2008) and recently also for pathology independent classifications (Dindorf et al., 2021a). In the static context, the system has been investigated in a series of studies and has proven to be valid and highly reliable in the estimation of segment-related spinal posture based on back surface information when compared with the clinical gold standard (x-ray imaging) (Krott, Wild, & Betsch, 2020; Mohokum et al., 2010; Mohokum, Schülein, & Skwara, 2015).

Meanwhile, ST is also applicable for the evaluation of spinal motion during gait due to technical and mathematical development. Its validity in marker detection and reproducibility in dynamic assessments has already been demonstrated (Betsch et al., 2011; Betsch et al., 2013; Gipsman, Rauschert, Daneshvar, & Knott, 2014). However, even though exploratory artificial intelligence (AI) -driven analyses were used to map gender differences (Dindorf et al., 2020) and to identify individuals based on dynamic ST data (Dindorf et al., 2021b), the dynamic ST measurement approach is still predominantly used for evaluations of global spine parameters (Gipsman et al., 2014; Michalik et al., 2019; Michalik et al., 2020). To the authors' knowledge, only one further article, which mainly focused on comprehensive visualization tools to facilitate data interpretation of ST measurements, presented data of isolated spinal movements of individual vertebrae in temporal relation to the gait cycle based on a small sample of 12 healthy participants (Haimerl et al., 2022).

Hence, the aim of this study was to present reference data for rotary spinal motion of every vertebral body from C7 down to L4 and the pelvis, derived from ST back shape analyses in a cohort of 201 healthy participants walking on a treadmill at a given walking speed of 5 km/h. Additionally, the spine's functional movement behavior during gait should be described in the transverse plane.

2. Methods

The present investigation followed the design of a prospective, explorative, cross-sectional study. Participants were included if they were aged 18 to 70 years, were free of pain at the moment of data collection and had no history of surgery or fracture between the spinal segments of C7 and the pelvis. They had no medical or therapeutic treatment due to spinal or pelvic girdle complaints (C7-pelvis) within the last 12 months and no medical or therapeutic treatment due to musculoskeletal problems (musculoskeletal system except C7-pelvis) within the last 6 months prior to the investigation. All participants had a body mass index (BMI) of $\leq$30.0 kg/m^2 (due to data capturing requirements), demonstrated an adequate gait stability (Timed-up-and-Go test (Bischoff et al., 2003)), an age- and sex-accorded walking speed (Two-Minute Walk test (Bohannon, Wang, & Gershon, 2015)) and spinal function (Back Performance Scale (Myklebust, Magnussen, & Inger Strand, 2009)) as well as an appropriate joint mobility to theoretically be able to perform a physiological gait pattern (Perry & Burnfield, 2010). The study was approved by the responsible ethics committee at the Rhineland-Palatinate Medical Association in Germany and is registered with the World Health Organization (WHO) (INT: DRKS00010834).

Based on a statistical sample size calculation, 201 healthy participants (sex ratio 2/3 to 1/3) were included who gave their informed consent prior to participation. Further details of participants' biometric characteristics are presented in Table 1. The sample size of n = 201 participants has been chosen to ensure sufficient accuracy for the limits of 95% reference ranges. It was planned to determine 95%

Table 1
Biometric characteristics of the included participants (n = 201).

Characteristics	Participants (n = 201)
Age (years):	
mean (±SD)	41.3 years (±13.4 years)
range	18–70 years
Sex (n):	
female (%)	n = 132 (65.7%)
male (%)	n = 69 (34.3%)
BMI (kg/m^2):	
mean (±SD)	23.5 kg/m^2 (±2.8 kg/m^2)
range	17.5–29.9 kg/m^2

reference ranges for all clinically relevant spinal parameters within each of the three planned age cohorts and to limit those reference ranges by 2.5% and 97.5% percentile curves. To ensure the reference range's width is not too large in direct proportion to the width of the confidence interval, a sample size of 66–67 participants per age cohort (young age cohort (18–30 years), middle age cohort (31–50 years) and old age cohort (51–70 years)) has been chosen, which resulted in a respective width-proportion of 0.175 (Troendle & Yu, 2003).

Data were captured using the ST DIERS formetric III 4D™ measuring device (software versions DICAM 3.7.1.7 for data collection and DICAM v3.5.0Beta11 for data export). The measurement approach is based on the principle of triangulation (Drerup, 2014). A slide projector is used as the optical equivalent to an inverse camera and projects horizontal and parallel lines on the unclothed back, while the participants are walking on a treadmill at a predefined distance from the measuring device. An additional camera system contemporaneously records the transformed line pattern (due to the participant's individual back surface curvatures) with a frequency of 60 Hz. By means of a software integrated algorithm, a three-dimensional scatter plot is created, which is comparable to a virtual plaster cast of the participant's individual back surface (consisting of up to 150,000 individual data points, depending on body size). Based on a clinically validated correlational model, the measuring system estimates the three-dimensional position of the underlying spinal segments continuously based on back surface information (Drerup, 2014; Drerup et al., 2001; Drerup & Hierholzer, 1994) (Fig. 1).

With a frequency of 100 Hz, a synchronized, treadmill-integrated foot pressure measuring system (Zebris FDM) enabled the automatic detection of initial and terminal contacts of the feet, required for later gait cycles analyses.

In contrast to static measurements, scattered reflective markers were required for dynamic analyses. For this reason, all participants were marked with seven reflective markers prior to data capturing (on the spinal process of C7, the spinous processes between the medial parts of the spinae scapulae (~T3) and the thoracolumbar transitions (~T12), the left and right posterior superior iliac spine (PSIS) and on both acromia). Palpation and marker attachments were always performed by the same investigator (physical therapist) following a standardized protocol for best possible control for potential palpation bias. To verify the correct placement of markers, a static control scan of the participant's back surface has been performed prior to data collection. In case of clinically inconclusive measurement results, marker placements had been checked, palpated again and corrected if necessary. Once the final position of markers was fixed, they were not changed for the duration of data collection.

To become familiar with the treadmill and the measuring environment, all participants completed a standardized warm-up procedure. They were asked to walk on the treadmill without using the handrail at a given walking speed of 3.5 km/h for 3 min. Afterwards the velocity was slowed down to 2 km/h and accelerated every 30 s by 1 km/h until the highest predefined walking speed (5 km/h) was reached and maintained for further 30 s.

During data collection, participants were barefoot and only wore short sports pants; the upper body was bare due to metrological reasons. Participants with long hair were asked to put their hair up, to allow the measurement system to detect the neck contour and the C7 marker. After a static scan in an upright standing position with eyes looking at a standardized point ~2 m away and 20 cm below each individual's body height, the three-dimensional vertebral body-related movement behavior was captured at four gait velocities (2 km/h, 3 km/h, 4 km/h and 5 km/h) in randomized order from every participant with the same standardization of viewing direction. Three complete gait cycles, starting with initial contact of the right foot, were recorded subsequently for a familiarization period of two minutes walking at the respective walking speed. Participants were not explicitly informed about the start of data recording after the familiarization period to ensure a preferably habitual gait performance.

In case of directly apparent software misinterpretations or other inconsistent, clinically not comprehensible measuring artifacts in evidence of the data output, the respective measurement has been repeated. After completion of the data collection phase, the investigator and an additional technician, who was highly familiar with the software and the measuring system, inspected all videos and the graphical data output visually for reasons of quality assurance, to check for further abnormal spinal movements or other measuring artifacts and to correct them if necessary.

Using a data export interface with the DICAM v3.5.0Beta11 software that was developed in close collaboration with the

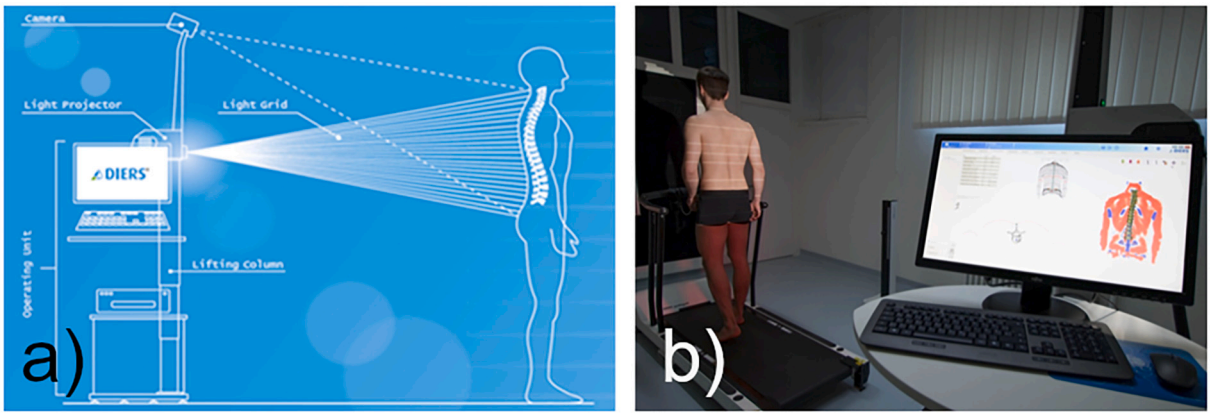

Fig. 1. a) Schematic illustration of the ST measurement device; b) ST measurement of a participant.

Table 2
Number of shifted values on the SGC-axis and the respective formula used.

	C7	T1	T2	T3	T4	T5	T6	T7	T8	T9	T10	T11	T12	L1	L2	L3	L4	Pel
Formula:	93	83	76	75	74	82	83	86	87	80	74	67	54	37	15	8	3	4
if value $\leq$ cut-off value, then + 101	(29)	(31)	(13)	(12)	(10)	(9)	(8)	(9)	(9)	(10)	(10)	(10)	(16)	(18)	(7)	(9)	(14)	(16)
Formula:	0	3	2	0	0	0	0	0	0	0	0	0	0	1	3	6	16	37
if value $>$ cutoff value, then − 101		(96)	(96)											(95)	(96)	(96)	(88)	(91)

Note. Cutoff values are presented in brackets ().

manufacturing company of the Formetric®-System (DIERS International GmbH) it was possible to export ST vertebral body-related raw data in all three dimensions, respectively, and in temporal relation to the actual phase of the gait cycle as .csv files from the DICAM software.

For data preprocessing, the Statistical Analysis System (SAS version 9.4) was used to standardize the data by transforming time stamps of measurements from seconds to the completed percentage of each individual gait cycle and averaging the results over all three recorded gait cycles. Due to the application of interpolating splines, smoothed and averaged data curves of measured rotation over gait cycle percentages were obtained for each individual vertebra and the pelvis. A regression model was used for interpolation of the individual's respective value for a scale reaching from 0 to 100 as a percentage (standardized gait cycle (SGC)). This allowed for the comparison of various data points of interest, irrespective of the individual's scale of the gait cycle. For the following descriptive analyses, the SGC of the right reference leg was evaluated at all integer percentage values between 0% and 100%, making it possible to compare the segment-related spinal movements between different individuals (Betz et al., 2018). Repositories, containing the respective SAS and SPSS scripts are accessible (Konradi, 2022a, 2022b, 2022c, 2022d; Schmidtmann & Konradi, 2022; Westphal & Konradi, 2022).

Because of the cyclical nature of gait cycle data, the distribution of each parameter of interest within the cycle had to be taken into account for further statistical analyses. This meant that for parameters that were distributed around the beginning and end of the gait cycle, the timescale was shifted in order to yield continuous distributions of these parameters. This was necessary, for example, for calculations of mean times within the gait cycle, e.g., in a situation where half the rotation maxima lay between 90% and 100% and the other half lay between 0% and 10%. The shift was done manually for each parameter and according to predefined rules. These contained that the largest gap between two different data points within the SGC data sets was defined for every analyzed vertebra and the pelvis and for both directions of movement (left and right rotation). Once the largest gap was found (at least $\geq$10 percentage values), it was used to divide the respective set of data into two groups. Depending on whether the majority of data points of the larger group were located within the first (0%–50%) or the second half (50%–100%) of the SGC, the data points of the smaller group were shifted by either adding or subtracting 101 percentage values on the x-axis to move them respectively to the end or to the beginning of the SGC. The chosen approach was deemed more efficient and reliable than implementing additional cyclical data analysis methods.

Afterwards, 95% prediction ellipses, mean values and the 2.5% and 97.5% percentiles were calculated for the respective sets of data. To enable a better traceability of the chosen approach, the x-axis (SGC) had been adjusted accordingly for the relevant graphical presentations (reaching now from −20% to 140%). Additionally, the number of affected values that had been shifted was indicated for the respective vertebrae and for both directions of movement (Table 2). Descriptive data analysis was performed using Statistical Package of the Social Sciences (SPSS version 23) and Microsoft Excel (version 2016).

To give a comprehensive overview across one dimension of movement, the following analyses and presentations of results will solely focus on vertebral body-related motion data from the transverse plane, as, on the one hand, this turned out to be the most difficult one to measure with the current commonly used motion capturing devices. On the other hand, ST transverse plane analyses

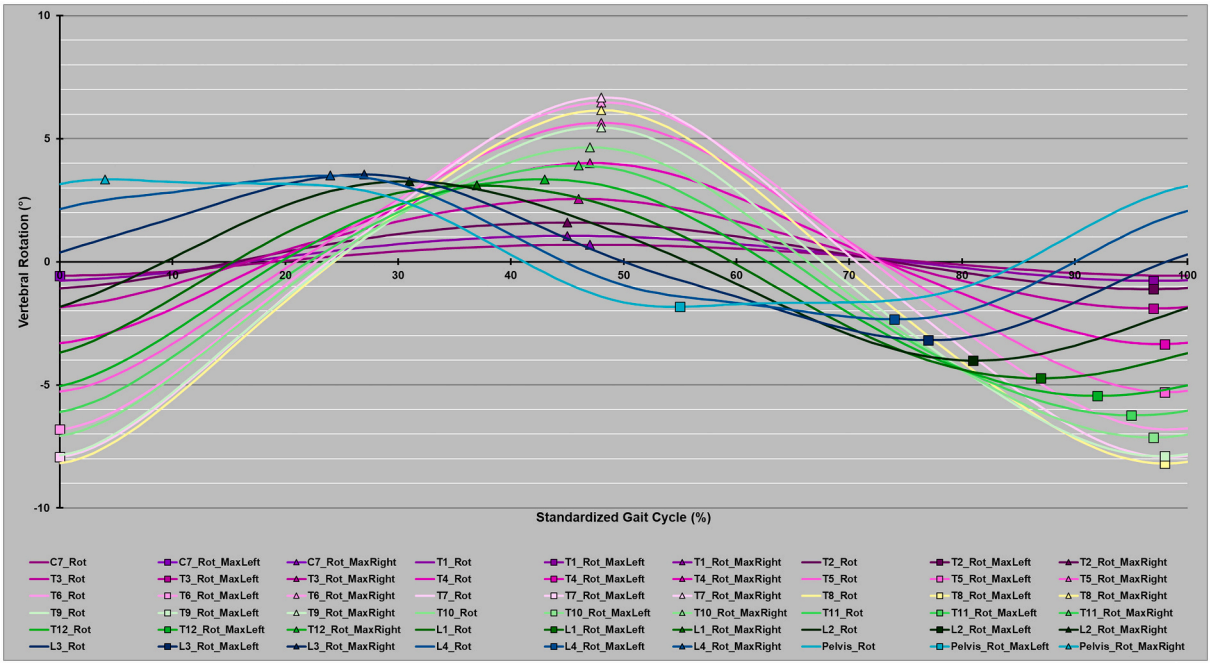

Fig. 2. Mean rotation curves of all investigated vertebrae and the pelvis within one SGC.
Note. Mean rotation curves are marked with their respective maximum of left (▲) and right (■) -side rotation (y-axis (−10°/+10°); x-axis (0%–100%)).

demonstrated the lowest standard error of the mean and therewith higher accuracy compared to the two other planes of movement for dynamic analyses in previous research (Gipsman et al., 2014). Additionally, evaluations will solely concentrate on data derived from a gait velocity of 5 km/h. Future analyses, however, will also address the remaining two axes of motion and the remaining measured gait velocities (2 km/h, 3 km/h and 4 km/h). Furthermore, subgroup analyses will look for possible differences in spinal motion patterns between male and female participants as well as between participants of different age cohorts within the presented study population. In addition, reference values for static spinal posture have recently been published based on the present set of data for the above-described subgroups as well (Huthwelker et al., 2022).

3. Results

For a gait velocity of 5 km/h, the mean curves of all investigated vertebrae and their respective maximum values of right- and left-side vertebral rotation within the SGC derived from 201 healthy participants are presented in Fig. 2. Fig. 3 shows the same data, but presents the averaged rotation of every investigated vertebra and the pelvis in anatomical order from cranial to caudal in a single SGC, respectively, in the style of the visualization approach from Haimerl et al. (2022).

For better interpretability and to address inter-individual variances, Fig. 4 and Video 1 show the isolated mean curve progressions of every investigated vertebra and the pelvis, complemented by the 2.5% and 97.5% percentile curves (for numerical displays see Table 3).

The graphical data output revealed almost sinusoidal curve oscillations for rotary spinal motion in all anatomic heights. Only one maximum for right- and left-side vertebral rotation can be seen within the SGC over all investigated vertebrae and for the pelvis itself. The mean curves, however, did not oscillate completely uniformly around 0° but were instead slightly shifted towards a negative (right side) vertebral rotation (Figs. 2 and 3; Video 1; Table 3).

In the cervicothoracic region, very little rotary motion was observed and maximum values could hardly be defined. Beginning with the third thoracic vertebra, the rotary amplitude of the respective oscillations started to increase and reached its largest extent around the mid-thoracic spine (T7 and T8). Afterwards, the extent of the rotary movement amplitude diminished again for the lower-lying vertebrae and for the pelvis itself. For the mid- and lower-thoracic spine the respective curves' apexes were clearly identifiable. The vertebrae of the lumbopelvic region, however, demonstrated a plateau formation for both sides of rotary curve progressions, making it more difficult to explicitly identify the respective curves' extreme values.

When looking at the time course of appearances of the movement curves' vertices, it can be seen that the pelvis reached its curve maximum almost at the beginning of the SGC (4%), as the first of all investigated structures. The overlying vertebrae until the lumbothoracic transition (L4–T12) followed in succession. The mid-thoracic vertebrae (T11–T3) achieved their maximum values almost simultaneously around 46%–48% of the SGC. For vertebral rotations to the other side, a comparable pattern could be observed (Figs. 2 and 4; Video 1; Table 3).

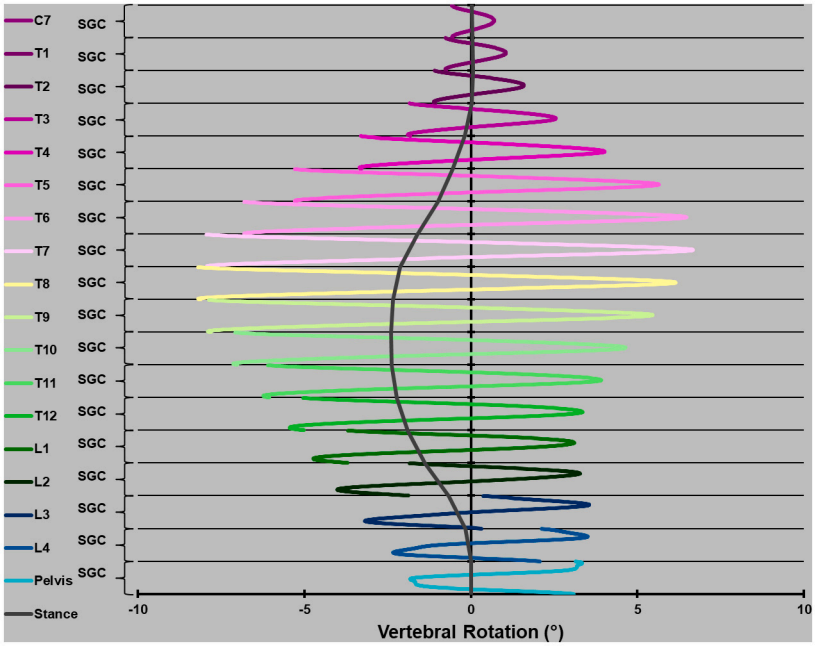

Fig. 3. Mean rotation curves of all investigated vertebrae and the pelvis within a single SGC respectively.
Note. Data is presented in the style of the visualization approach from Haimerl et al. (2022). The mean transverse plane results for spinal posture during stance are additionally presented. In contrast to dynamic results from gait analyses, the DIERS system provides static results from posture analyses for each vertebral structure during stance measurements in relation to a neutral pelvic position (Wolf et al., 2021).

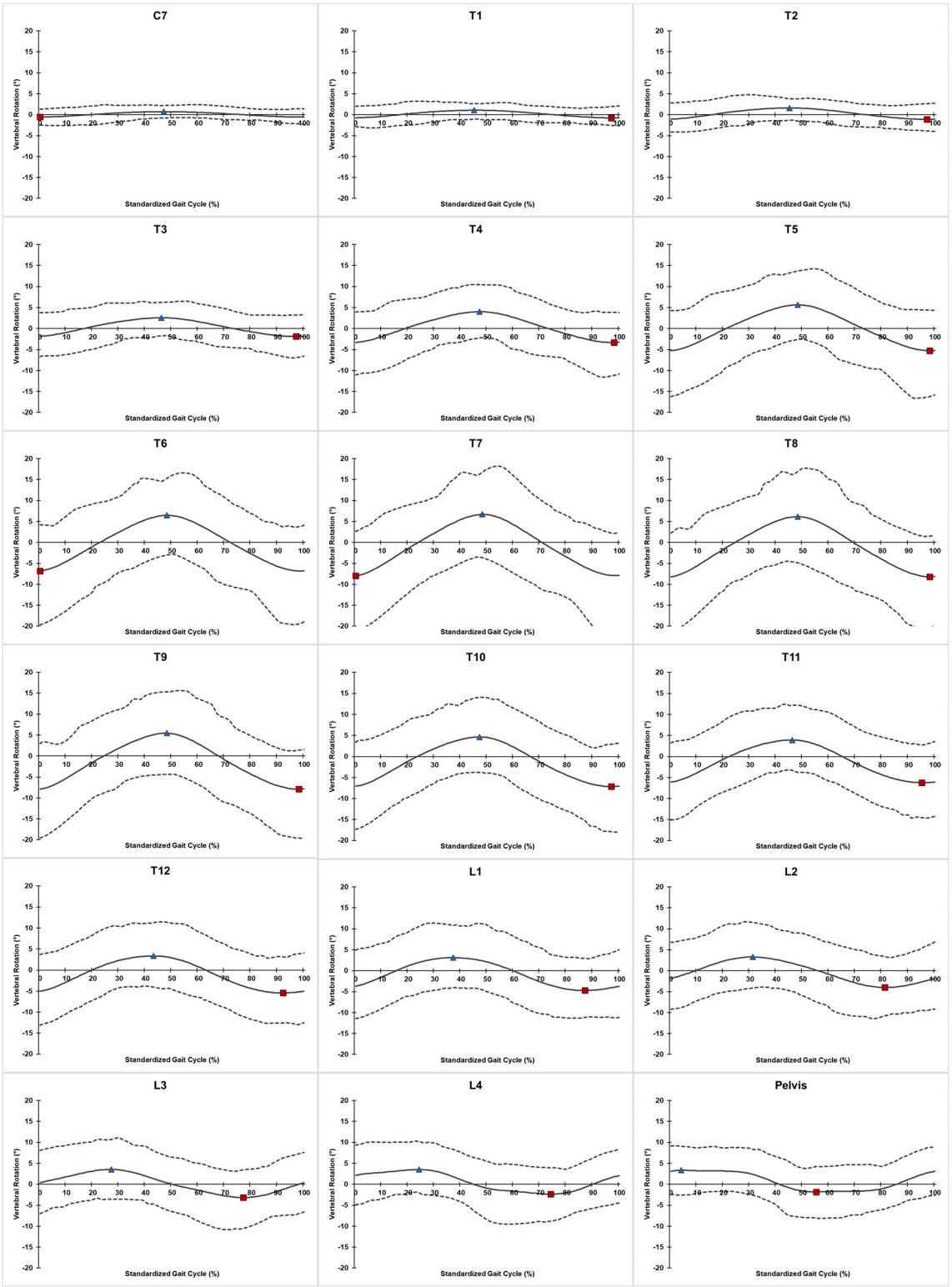

Fig. 4. Mean rotation curves and their respective 2.5% and 97.5% percentile curves of every vertebra and the pelvis (C7–L4; pelvis) within the SGC. *Note.* Vertebral rotation (°) is represented on the y-axis (range: −25°/+25°), the time progression of the SGC is represented on the x-axis (0–100%). Mean rotation curves are covered by their respective 2.5% and 97.5% percentile curves**.** The mean's maximum vertebral rotation values to the left (▲) and to the right (■) side are highlighted.

Table 3
Maximum values of the mean curves across the SGC with their respective 2.5% and 97.5% percentiles and the associated time of appearance within the SGC.

	Time within SGC (%)	Max of Mean Rot Right (°)	2.5% Pctl (°)	97.5% Pctl (°)	Time within SGC (%)	Max of Mean Rot Left (°)	2.5% Pctl (°)	97.5% Pctl (°)	Range of Rotary motion (°)
C7	0	−0.6	−2.5	1.3	47	0.7	−0.8	2.3	1.3
T1	97	−0.8	−2.6	2.0	45	1.1	−1.1	2.7	1.8
T2	97	−1.1	−3.9	2.6	45	1.6	−1.3	3.8	2.7
T3	97	−1.9	−6.9	3.2	46	2.6	−1.7	6.2	4.4
T4	98	−3.3	−11.1	3.9	47	4.0	−2.2	10.5	7.4
T5	98	−5.3	−16.2	4.4	48	5.7	−2.6	13.7	10.9
T6	0	−6.8	−19.7	4.1	48	6.5	−3.0	15.3	13.3
T7	0	−7.9	−21.3	2.6	48	6.7	−3.7	16.7	14.6
T8	98	−8.2	−20.3	1.5	48	6.2	−4.9	16.9	14.4
T9	98	−7.9	−19.6	1.4	48	5.5	−4.4	15.3	13.4
T10	97	−7.1	−17.9	2.9	47	4.6	−3.8	14.1	11.8
T11	95	−6.2	−14.5	2.7	46	3.9	−3.3	12.2	10.2
T12	92	−5.4	−12.6	3.2	43	3.3	−4.1	11.3	8.8
L1	87	−4.7	−11.1	3.0	37	3.1	−4.1	10.8	7.8
L2	81	−4.0	−10.8	3.4	31	3.3	−4.1	11.5	7.3
L3	77	−3.2	−10.5	3.5	27	3.5	−3.6	10.7	6.7
L4	74	−2.3	−8.8	4.0	24	3.5	−2.0	10.2	5.8
Pelvis	55	−1.8	−8.1	4.2	4	3.3	−2.6	9.1	5.2

Due to these findings, the point of intersection (PoI), meaning the area of transition where the vertebral rotation changes its direction (from right- to left-side vertebral rotation and vice versa) and around which the spinal screwing occurs, was not found to be static around the area of the mid-thoracic spine (Fig. 5; Video 2).

At the beginning of the SGC, the PoI was located between the 3rd and the 2nd lumbar vertebra (Figs. 2 and 5; Video 2). With the progression of the SGC over time, it moved upwards in its anatomic localization from one vertebra to the next until the anatomic height of T9/T10. Afterwards a time interval occurs, in which all vertebrae were rotated into the same direction and where no PoI could be observed (Figs. 2 and 5; Video 2). Initiated by the pelvis's change of rotary motion to the opposite direction, all other vertebrae

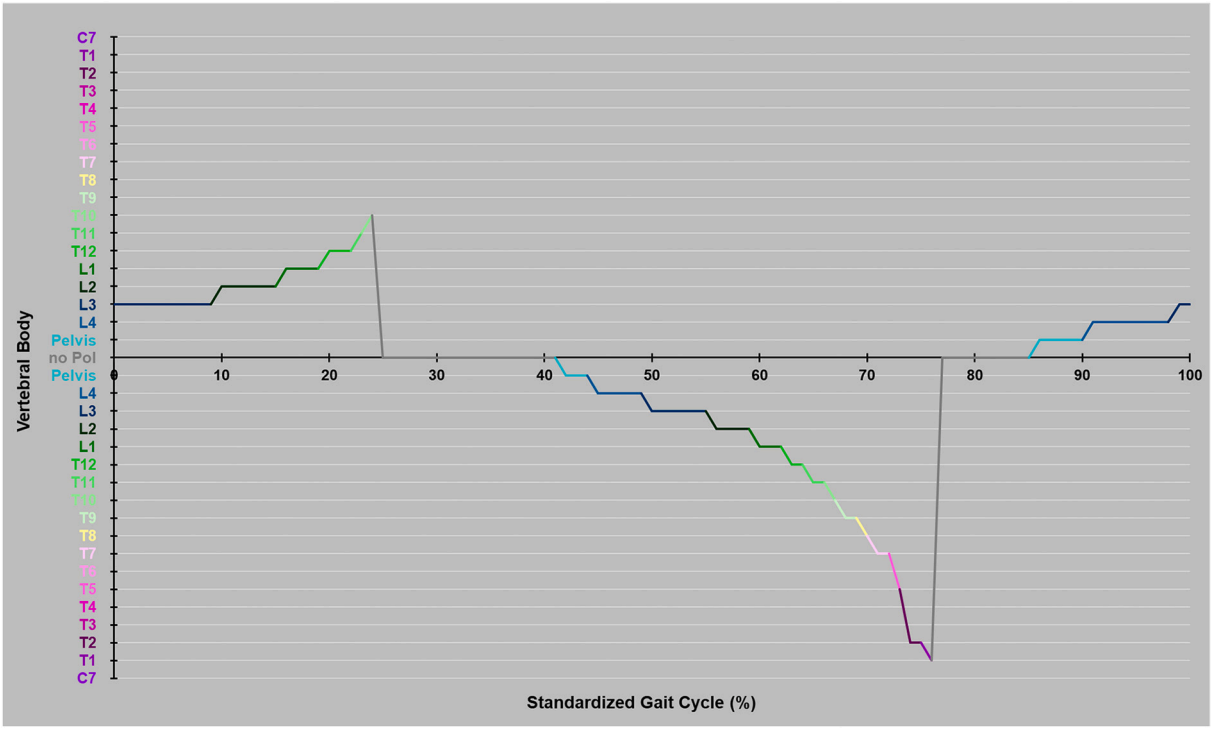

Fig. 5. Progression of the PoI within the SGC.
Note. As the PoI always occurs between two adjacent vertebrae, the respective caudal vertebra is marked as the PoI in this figure.

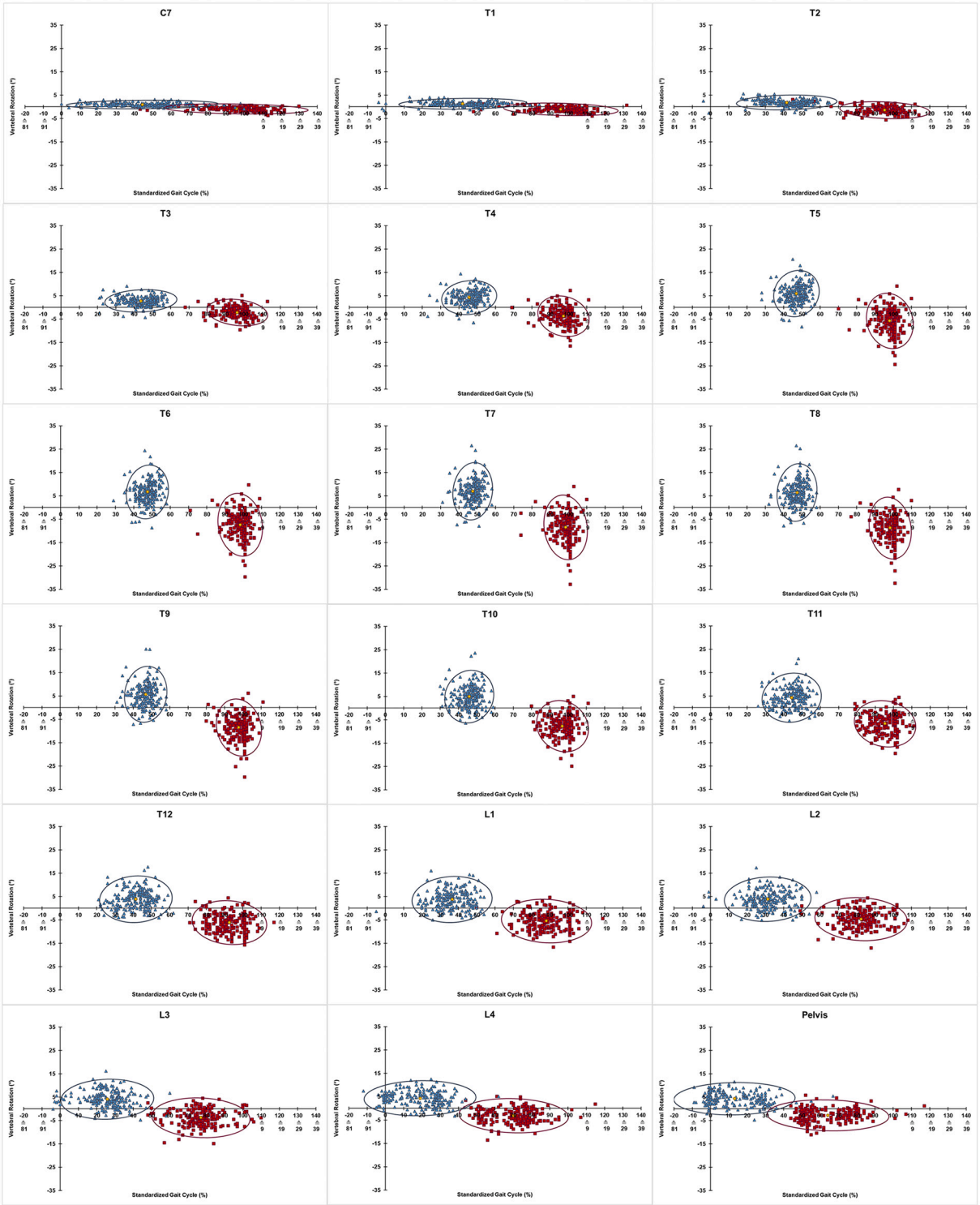

Fig. 6. Distribution of individual values (n = 201) for maximum vertebral rotation to the right (■; red) and to the left side (▲; blue) for all investigated vertebrae and the pelvis.

Note. Rotary vertebral motion (°) is represented on the y-axis (range: −35°/+35°), the time of occurrence within the SGC is represented on the x-axis (range: -20%/+140%). Scatter plots are covered by the 95% prediction ellipses for right- and left-side vertebral rotation, respectively. The center of the ellipses are marked (●; yellow). (For interpretation of the references to colour in this figure legend, the reader is referred to the web version of this article.)

followed in succession. The period of no PoI ended at that moment when the extent of rotary motion of the pelvis crossed the neutral position (0° of rotary motion on the y-axis) at around 42% of the SGC (Figs. 2 and 5; Video 2; Table 3). At this moment, the PoI appeared caudal, between the pelvis and the 4th lumbar vertebra and again started to increase gradually, vertebra by vertebra until all investigated structures were rotated into the same direction again and no PoI can be located. Even before all vertebral bodies have crossed the neutral rotary position, the pelvis had already started to initiate the next change of rotary direction and crossed the x-axis at around 86% of the SGC (Figs. 2 and 5; Video 2). In consequence, the PoI appeared caudal again between the pelvis and the 4th lumbar vertebra. As before, it increased slightly until the anatomic level of L3/L2 was achieved at the end of the SGC.

Even though mean results of the entire group demonstrated those very systematic spinal movement patterns, individual observations revealed large inter-individual differences in vertebral movement habits during gait. Fig. 6 and Video 3 present the distribution of individual rotational maximum values of all 201 participating subjects within the SGC. The presented scatter plots of individual values are framed by their respective 95% prediction ellipses, meaning that with a probability of 95% the ellipse is able to cover a respective future observation (Schubert & Kirchner, 2014). The pelvis and the lower lumbar vertebrae demonstrate that, compared to their considerable homogeneous distribution on the y-axis (range of vertebral rotation), the temporal occurrence of individual maximum values spreads widely on the x-axis (% SGC), which is also visible in the ratio of the ellipses length to its width. In contrast, the mid- and lower-thoracic vertebrae demonstrate the almost opposite movement behavior. They provide quite homogeneous patterns for timely occurrence of the individual maximum values within the SGC. The distribution of values on the y-axis, however, revealed quite heterogeneous results. The area of the prediction ellipse, which is defined to be the product of its principal axes with pi (Schubert & Kirchner, 2014), tends to increase from the cranial to the caudal structures, indicating in general a more heterogeneous movement behavior of the caudal compared to the cranial vertebrae (Fig. 6; Video 3; Table 4). The mean values and their respective 2.5% and 97.5% percentiles for temporal occurrence of right- and left-side maximum rotation within the SGC and the corresponding rotation values are presented in Table 5.

4. Discussion

The aim of this study was to present reference data for rotary spinal motion of every vertebral body from C7 down to L4 and the pelvis derived from ST back shape analyses in a cohort of 201 healthy participants walking on a treadmill at a given walking speed of 5 km/h. Additionally, the spine's functional movement behavior during gait should be described in the transverse plane.

The vertebrae of the cervicothoracic region demonstrated no notable range of rotary motion (rRoM) (rRoM C7 = 1.3°, rRoM T1 = 1.8°, rRoM T2 = 2.7°). Additionally, the respective prediction ellipse areas were also relatively small, indicating more homogeneous movement patterns compared to those of the underlying spinal structures. This was expected because, in general, the human body seems to be striving to stabilize the head during walking (Kavanagh, Barrett, & Morrison, 2006). The standardization of viewing direction on a fixed point at a predefined height and distance from the walking participant might also have contributed to this outcome.

Based on the made observations of the underlying vertebrae, however, the current results challenge the existing functional understanding of vertebral body-related rotary motion of the healthy spine during gait. So far, the mid-thoracic spine (~T7) was mostly expected to be dynamically stabilized, demonstrating no or rather little rotary motion during ambulation in healthy participants at all

Table 4
Numerical presentation of the 95% prediction ellipses for maximum values of right- and left-side vertebral rotation.

	Maximum of right-side vertebral rotation					Maximum of left-side vertebral rotation				
	Center of the ellipse		Length of the ellipse	Width of the ellipse	Area of the ellipse	Center of the ellipse		Length of the ellipse	Width of the ellipse	Area of the ellipse
	SGC-axis	Rotation-axis				SGC-axis	Rotation-axis			
C7	95.8	−0.9	39.3	2.1	258.1	44.2	1.0	41.6	1.8	238.4
T1	95.8	−1.1	31.3	2.6	254.7	42.0	1.4	35.0	2.3	254.2
T2	95.3	−1.4	24.6	3.6	276.7	41.7	1.9	27.5	3.2	272.9
T3	96.5	−2.2	16.7	5.6	292.0	43.7	2.8	19.7	4.8	296.2
T4	97.3	−3.7	14.2	8.5	379.2	45.6	4.3	15.1	7.2	341.4
T5	98.1	−5.8	13.2	11.4	472.5	47.0	5.9	12.6	9.8	386.3
T6	98.3	−7.4	13.8	11.8	513.2	47.5	6.8	12.0	10.9	413.9
T7	98.5	−8.5	14.1	11.7	516.7	47.6	7.0	12.5	10.7	417.1
T8	98.3	−8.8	13.5	11.2	475.1	47.3	6.4	12.5	10.7	419.6
T9	97.8	−8.5	13.1	11.5	470.8	46.8	5.8	12.4	11.2	435.8
T10	96.9	−7.7	14.3	10.8	484.4	45.9	5.0	13.5	11.2	473.1
T11	95.4	−6.9	16.9	9.8	521.9	44.3	4.3	16.2	10.5	533.3
T12	92.6	−6.1	20.5	9.3	598.7	41.5	3.9	19.9	10.0	623.2
L1	88.2	−5.5	24.6	9.3	720.6	36.6	3.8	22.0	9.9	679.4
L2	82.4	−4.7	25.3	9.2	731.8	31.3	3.9	23.7	9.5	706.9
L3	77.1	−3.8	26.9	8.4	712.9	25.8	4.1	25.5	8.5	682.6
L4	70.2	−3.1	29.9	7.3	688.3	19.0	4.3	30.7	7.5	725.2
Pelvis	64.3	−2.8	33.4	6.6	696.4	13.2	4.3	33.2	6.9	718.3

Note. Ellipses are described based on their length, width and area.

Table 5
Mean values and their respective 2.5% and 97.5% percentiles for temporal occurrence (Mean Max Rot (% SGC)) and the corresponding rotational deflection (Mean Max Rot (° Rot) of right and left side maximum vertebral rotation values.

	Right-side vertebral rotation						Left-side vertebral rotation					
	Mean Max Rot Right (% SGC)	2.5% Pctl (% SGC)	97.5% Pctl (% SGC)	Mean Max Rot Right (° Rot)	2.5% Pctl (° Rot)	97.5% Pctl (° Rot)	Mean Max Rot Left (% SGC)	2.5% Pctl (% SGC)	97.5% Pctl (% SGC)	Mean Max Rot Left (° Rot)	2.5% Pctl (° Rot)	97.5% Pctl (° Rot)
C7	95.8	48.2	120.0	−0.9	−2.7	0.6	44.2	10.1	80.9	1.0	−0.4	2.9
T1	95.8	55.4	115.9	−1.1	−3.2	1.0	42.0	13.0	67.0	1.4	−0.8	3.4
T2	95.3	71.1	109.0	−1.4	−4.4	1.7	41.7	18.1	59.0	1.9	−1.2	4.8
T3	96.5	79.1	106.0	−2.2	−7.4	2.9	43.7	23.2	56.0	2.8	−1.6	7.2
T4	97.3	83.1	105.0	−3.7	−11.7	3.2	45.6	33.0	56.0	4.3	−2.0	10.5
T5	98.1	85.1	106.0	−5.8	−16.6	3.7	47.0	35.1	56.0	5.9	−2.5	14.2
T6	98.3	87.0	106.0	−7.4	−19.8	3.3	47.5	36.1	56.0	6.8	−2.8	16.6
T7	98.5	87.1	106.0	−8.5	−21.3	2.1	47.6	38.0	55.0	7.0	−3.3	18.3
T8	98.3	87.1	106.0	−8.8	−21.0	1.3	47.3	37.0	55.0	6.4	−4.4	17.9
T9	97.8	84.1	106.0	−8.5	−19.8	1.2	46.8	34.1	55.0	5.8	−4.3	17.0
T10	96.9	83.0	106.0	−7.7	−18.1	1.9	45.9	33.0	55.0	5.0	−3.8	14.7
T11	95.4	80.1	107.0	−6.9	−15.2	1.8	44.3	29.1	57.0	4.3	−2.5	13.2
T12	92.6	77.1	107.0	−6.1	−13.6	2.0	41.5	24.0	56.0	3.9	−3.3	12.8
L1	88.2	69.0	105.0	−5.5	−12.1	2.3	36.6	19.1	52.0	3.8	−3.2	12.1
L2	82.4	59.0	102.0	−4.7	−11.8	2.9	31.3	12.1	50.0	3.9	−3.6	11.8
L3	77.1	51.1	102.0	−3.8	−10.9	2.4	25.8	−2.0	46.9	4.1	−2.8	11.3
L4	70.2	48.1	94.9	−3.1	−9.8	2.4	19.0	−3.0	39.0	4.3	−1.8	10.5
Pelvis	64.3	46.1	89.0	−2.8	−8.1	2.0	13.2	−4.0	37.9	4.3	−0.9	9.5

(Gregersen & Lucas, 1967; Needham, Naemi, et al., 2016; Suppé & Bongarz, 2013). The vertebrae above, respectively, the vertebrae and the pelvis below tended to be almost counterrotated depending on walking speed (Gregersen & Lucas, 1967; Lamoth, Beek, & Meijer, 2002). ST back shape analyses however, found the pelvis to be forwardly rotated on the side of the reference leg, reaching its curve maximum as the first of all investigated anatomic structures within the SGC (rRoM Pelvis = 5.2°). The maxima of the overlying lumbar vertebrae followed in succession. Instead of being adjusted in an almost neutral position, the vertebrae of the mid-thoracic spine were almost maximally counterrotated at the beginning of the SGC. Approximately halfway through the gait cycle the directions of maximum rotary movement reversed. Of all thoracic vertebrae, T7 and T8 demonstrated the largest amplitude of rotary motion during gait at a continuous velocity of 5 km/h (rRoM T7 = 14.6°, rRoM T8 = 14.4°). In addition, the largest rotary opposition was also found between the pelvis and T7/T8. Furthermore, the thoracic spine turned out to rotate in terms of a functional unit whereby all included vertebrae almost contemporaneously rotated into the same direction by the same period only with different amplitudes for the rotary RoM. Conversely, the segments of the pelvis and the lumbar spine seem to rotate successively but with almost identical rotary motion amplitudes.

Contrary to previous assumptions, the analysis of the present data additionally indicates that the mid-thoracic spine (~T7) might possibly not be an almost static point of intersection (PoI) where the direction of rotary motion changes from one side to the other and around which the spinal screwing occurs during ambulation. It rather looks as if the PoI seems to be dynamic in its anatomic localization during the course of the SGC, following a systematic and relatively constant from-caudal-to-cranial oscillation pattern (Fig. 5; Video 2). It may be conjectured that a dynamical PoI is a consequence of the human body increasing the degrees of freedom and simultaneously minimizing leverages to address the ability to be more resilient towards internal and external perturbations during the complex motion pattern of gait.

Comparable to the presented mean curves (specifically to those representing the rotary motion of the thoracic vertebrae), which oscillated not completely uniformly around the x-axis (0° of rotation) and which were slightly shifted downwards on the y-axis (Figs. 2, 3 and 4; Video 1), the course of the PoI revealed two different progressions within the SGC that showed an uneven increase of its anatomic localization between the first and the second rise (Fig. 5; Video 2). This phenomenon might be caused by the fact that the normal, non-scoliotic spine also demonstrates a pre-existing pattern of vertebral rotation, especially in the thoracic segments in consequence of internal organ anatomy and location (Kouwenhoven et al., 2007; Kouwenhoven, Vincken, Bartels, & Castelein, 2006). This predominant rotation was verifiable in static ST analyses of 100 female participants from the study cohort described within this paper as well (Wolf et al., 2021) and is also present in all 201 participants (stance graph in Fig. 3) (Huthwelker et al., 2022). However, as data of the current project were not normalized for the individual's habitual stance, this pre-existing rotation might have influenced the slightly asymmetrical rotary movement behavior between left and right vertebral rotation and therewith might also have affected the uneven progression of the PoI between left and right vertebral rotation. These findings seem to indicate that every individual walks systematically "around" his or her personal spinal posture, but future research needs to address this topic in more detail. Nevertheless, the described findings of a dynamic PoI that starts caudal and systematically rises upwards, reveals that the pelvis plays a very important role in transverse plane spinal motion during gait. It appears to actually initiate spinal rotary motion, while the overlying vertebrae "only" seem to follow the pelvis's movement in succession. Whether this pattern is dependent on gender, age or other contributing factors like walking speed will be analyzed and discussed elsewhere in further publications on this topic. Future analyses will also have to answer the question of whether the PoI's progression might differ between patient groups suffering from different

musculoskeletal pathologies, and in this case, whether its progression might be a reliable indicator to differentiate between physiological and pathological spinal movement patterns in the future.

The current study also found that rotary movement patterns during ambulation turned out to be much more individual than primarily expected, and that this heterogeneity increased from the cranial to the caudal spinal structures. This phenomenon could be observed, even though all participants were free of pain and healthy with regard to the musculoskeletal system, the procedure of data capturing was strictly standardized, and walking speed could be perfectly controlled for. These findings are in accordance with results of previous research regarding the individuality of gait patterns of the pelvic-leg region. Previous authors found that movement patterns of the lower extremity are quite individual and could differ so strongly from one subject to another that the respective gait characteristics can be used to recognize an individual reliably (Horst et al., 2016; Horst, Lapuschkin, Samek, Muller, & Schollhorn, 2019; Schöllhorn, Nigg, Stefanyshyn, & Liu, 2002). Additionally, it could be shown that those individual gait characteristics were persistent over years (Horst, Mildner, & Schollhorn, 2017). Whether this is also the case for movement patterns of the spine needs to be further investigated. Initial results using AI, however, indicate in this direction (Dindorf et al., 2021b).

Due to huge methodological differences in data capturing approaches, and different ways for data preparation in previous research investigating spinal dynamics during gait by using other measurement techniques, direct comparisons between previous findings and the results of the current study are hardly possible. To the authors' knowledge, this is additionally the first study presenting reference data for rotary spinal motion from all vertebrae (C7 to L4 and the pelvis) derived from healthy participants and in temporal relation to a standardized gait cycle using an ST measurement approach. Indeed, two further research groups previously used ST on healthy participants as well, but either focused on the presentation of global spine parameters (Michalik et al., 2020) or on the development of comprehensive new visualization tools (Haimerl et al., 2022). Even though Haimerl et al. (2022) did not present mean values for respective vertebral rotations of their study cohort, data visualizations of axial rotation revealed quite comparable movement patterns. The authors found the vertebral bodies to not oscillate even around 0°. Additionally, the vertebrae of the mid-thoracic spine seem to present the largest range of rotary motion, comparable to the results of the current study. Nevertheless, it has to be considered that individual data were presented from only 12 participants and for a walking speed of 3 km/h (Haimerl et al., 2022), which is why direct comparisons with results of the current study have to be interpreted with caution. For this reason, future research will have to evaluate the results presented herein and compare them in detail against prospective research findings.

4.1. Limitations

The presented study had several limitations. Thereby a distinction must be made between different methodological causes and limitations derived from the measurement method itself.

4.1.1. Methodological limitations

All participants included in the study were healthy, free of pain and did not show any functional abnormalities in relation to the inclusion criteria described. However, spinal health was not further verified by radiographic images due to ethical reasons. For this reason, the existence of small spinal deformities or other asymptomatic degenerative adaptations cannot be excluded.

Additionally, it has to be considered that the researchers decided to use two more markers (~T3 and ~ T12) than officially recommended by the manufacturer. This was to minimize systematic software misinterpretations for positions of individual vertebral bodies at the respective anatomical heights that frequently occurred during test measurements at fast walking speeds due to soft tissue motion on the participants' back surface. Additionally, C7 and the PSIS were palpated and marked instead of the recommended, visually identifiable landmarks (vertebra prominens and lumbar dimples). This approach was used because the recommended visual landmarks were not always identifiable on every participant's back surface. In such cases, the manufacturer recommends palpating and marking the respective anatomic landmarks anyway. As the researchers strived to standardize the measuring procedure as much as possible, they decided to mark the anatomic structures a priori for all participants. Nevertheless, the chosen approach was definitely more prone to palpation bias (Cooperstein & Hickey, 2016; Póvoa, Ferreira, Zanier, & Silva, 2018) and limits the external validity of the presented findings. Additionally, the divergent marking of landmarks might have influenced reconstructions of the virtual spinal model and consequently might have had an effect on the generated outcome for spinal rotary motion.

A further attempt to standardize the data capturing procedure as much as possible within the current study was the decision to analyze the participants' spinal motion based on predefined walking speeds. The researchers are aware that individual anthropometrics have an influence on biomechanical gait parameters (McKay et al., 2017) and that normal differences in comfortable gait speeds according to sex, age and height (Bohannon, 1997) have not taken into account. This has to be considered when transferring the here presented results into clinical practice.

The age of the participants included in this study ranged from 18 to 70 years. As age-related changes in spinal and lower limb movement patterns are known during gait (Crawford, Gizzi, Dieterich, Ni Mhuiris, & Falla, 2018), the wide age-range might have possibly contributed to the high inter-individual variance of gait patterns that occurred in the presented results. Further planned publications will analyze the available data with regard to sex, different age cohorts and different walking speeds (2 km/h, 3 km/h, 4 km/h and 5 km/h) to provide further clarity on the possible impact that those contributing factors might have had on individual gait performances.

Even though no explorative statistical analyses have been performed, multiple descriptive analyses of the same data set limits its statistical significance as the data are correlated. This has to be considered when the presented results are consulted in clinical practice.

A further weakness of the presented study is that the authors missed to capture the required number of performed manual data corrections. The lack of this information limits the interpretability of the results in a wider context and has to be considered when

results shall be transferred into clinical practice.

Furthermore, during a short period of time (16–24% of the SGC) more than one PoI was apparent in the available set of data (Video 2). As the additional PoIs were located in the upper-thoracic spine, where only very little rotary motion was observed anyway, and because they were only apparent for a very short time, the authors waived picturing these additional data for reasons of a better interpretability of the graphical PoI visualization.

4.1.2. Limitations that arised from the measurement method itself

To date, it is not possible to properly validate the dynamic ST measurement approach due to the absence of a suitable clinical gold standard for spinal motion analysis to compare it against. Therefore, the results from dynamic ST analyses still derive from optical back shape recordings via a mathematical algorithm that was originally developed and validated for static measurements. Additionally, arising soft tissue artifacts caused by scapula motion on the thorax, back muscle activation, general skin displacements or skin stretching over the spinal processes during motion might have had an influence on the measured data that also has to be considered when interpreting and using the presented results for clinical or scientific practice.

Furthermore, only participants with a BMI $\leq$30.0 kg/m^2 were included in the study. This approach was chosen, due to data capturing requirements, knowing that this further limits the external validity of the presented outcome.

An additional point for consideration is that for ST measurements, it is required to hold the distance between the measuring device and the walking participant approximately constant during the time of data recording. This is why participants had to walk on a treadmill for data capturing within this study. Whether this is equal to walking overground or not, has been a much debated research question for many years. In this context, a recent systematic review found that while some biomechanical parameters are largely comparable between treadmill and overground walking, others were significantly different from each other (Semaan et al., 2022). Nevertheless, the laboratory conditions themselves will definitely have had an influence on the participants' gait performance compared to daily life walking, regardless of whether the participants were analyzed on a treadmill or on any other surface.

Last but not least, it is necessary to question whether three recorded gait cycles are representative of an individual's habitual gait performance. This approach has been chosen due to a high amount of data generated with the ST measuring device on the one hand, and indeed generous but still limited data storage capacities on the other. However, as already published ST measurement results indicated, spinal movement patterns, derived from identical three-gait-cycle ST analyses seem to be quite constant and reproducible over time (Dindorf et al., 2021b), the results of this approach seem nevertheless meaningful and suitable.

4.2. Outlook for future research

To the authors' knowledge, this is the first presentation of reference data of vertebral body-related rotary movement behavior of the healthy human spine during gait, collected with an ST measurement device. Future analyses of the current set of data will have to provide further information on spinal movement behavior in the remaining axes of motion (frontal and sagittal) and for the additionally measured gait velocities (2 km/h, 3 km/h and 4 km/h), which will be presented in further publications. Furthermore, the questions of whether the variety of spinal movement patterns is intra-individually consistent and whether it is affected by an individual's physical constitution, sex, anthropometric characteristics, age, walking speed or by other contributing factors will have to be addressed.

Additionally, future research will have to develop characteristic parameters to describe specific spinal gait patterns based on ST data. Those parameters should be able to differentiate between physiological and pathological movement patterns. AI methods might be able to further facilitate this process (Horst et al., 2019) and have already been used with promising results on the presented data set so far (Dindorf et al., 2020; Dindorf et al., 2021b).

Supplementary data to this article can be found online at https://doi.org/10.1016/j.humov.2022.103054.

Funding sources

The research did not receive any specific grant from funding agencies in the public, commercial, or not-for-profit sectors.

There was various technical assistance by staff members of the DIERS Company in preparation prior to the statistical data analysis process. However, there was no external influence on the study design, in the collection, statistical analysis and interpretation of data, in the writing of the manuscript, and in the decision to submit the manuscript for publication.

CRediT authorship contribution statement

Janine Huthwelker: Conceptualization, Methodology, Validation, Formal analysis, Investigation, Data curation, Writing – original draft, Visualization. **Jürgen Konradi:** Software, Validation, Formal analysis, Data curation, Writing – review & editing, Visualization, Supervision, Project administration. **Claudia Wolf:** Software, Validation, Formal analysis, Data curation, Writing – review & editing. **Ruben Westphal:** Software, Validation, Formal analysis, Data curation, Writing – review & editing. **Irene Schmidtmann:** Software, Validation, Formal analysis, Data curation, Writing – review & editing. **Patric Schubert:** Validation, Formal analysis, Data curation, Writing – review & editing, Visualization. **Philipp Drees:** Resources, Writing – review & editing, Supervision, Project administration. **Ulrich Betz:** Conceptualization, Methodology, Validation, Resources, Writing – review & editing, Supervision, Project administration.

Declaration of Competing Interest

None.

Data availability

The authors do not have permission to share data.

Acknowledgements

First and foremost we would like to thank all participants for their interest and their time to participate in this project. Our colleagues are acknowledged for their immense support within the participant recruitment process and for their professional expertise and contributions to this project. Special thanks also to Amira Basic and Kjell Heitmann (DIERS Company) for their technical support and assistance.

References

Betsch, M., Wild, M., Johnstone, B., Jungbluth, P., Hakimi, M., Kuhlmann, B., & Rapp, W. (2013). Evaluation of a novel spine and surface topography system for dynamic spinal curvature analysis during gait. *PLoS One, 8*(7), Article e70581. https://doi.org/10.1371/journal.pone.0070581

Betsch, M., Wild, M., Jungbluth, P., Hakimi, M., Windolf, J., Haex, B., … Rapp, W. (2011, Jun). Reliability and validity of 4D rasterstereography under dynamic conditions. *Computers in Biology and Medicine, 41*(6), 308–312. https://doi.org/10.1016/j.compbiomed.2011.03.008

Betz, U., Konradi, J., Huthwelker, J., Wolf, C., Diers, H., Heitmann, K., Westphal, R., & Drees, P. (2018). *Quantitative and qualitative parameters to characterize segmental spine movement during gait World Congress of Biomechanics, Dublin, Ireland*, 2018.07.08-12.

Bischoff, H. A., Stahelin, H. B., Monsch, A. U., Iversen, M. D., Weyh, A., von Dechend, M., … Theiler, R. (2003, May). Identifying a cut-off point for normal mobility: A comparison of the timed "up and go" test in community-dwelling and institutionalised elderly women. *Age and Ageing, 32*(3), 315–320. https://doi.org/10.1093/ageing/32.3.315

Bohannon, R. W. (1997, Jan). Comfortable and maximum walking speed of adults aged 20-79 years: Reference values and determinants. *Age and Ageing, 26*(1), 15–19. https://doi.org/10.1093/ageing/26.1.15

Bohannon, R. W., Wang, Y. C., & Gershon, R. C. (2015, Mar). Two-minute walk test performance by adults 18 to 85 years: Normative values, reliability, and responsiveness. *Archives of Physical Medicine and Rehabilitation, 96*(3), 472–477. https://doi.org/10.1016/j.apmr.2014.10.006

Bruijn, S. M., Meijer, O. G., van Dieen, J. H., Kingma, I., & Lamoth, C. J. (2008, Apr). Coordination of leg swing, thorax rotations, and pelvis rotations during gait: The organisation of total body angular momentum. *Gait & Posture, 27*(3), 455–462. https://doi.org/10.1016/j.gaitpost.2007.05.017

Ceccato, J. C., de Seze, M., Azevedo, C., & Cazalets, J. R. (2009, Dec 7). Comparison of trunk activity during gait initiation and walking in humans. *PLoS One, 4*(12), Article e8193. https://doi.org/10.1371/journal.pone.0008193

Chockalingam, N., Dangerfield, P. H., Giakas, G., & Cochrane, T. (2002). Study of marker placements in the back for opto-electronic motion analysis. *Studies in Health Technology and Informatics, 88*, 105–109.

Cooperstein, R., & Hickey, M. (2016, Mar). The reliability of palpating the posterior superior iliac spine: A systematic review. *The. Journal of the Canadian Chiropractic Association, 60*(1), 36–46.

Crawford, R., Gizzi, L., Dieterich, A., Ni Mhuiris, Á., & Falla, D. (2018). Age-related changes in trunk muscle activity and spinal and lower limb kinematics during gait. *PLoS One, 13*(11), Article e0206514. https://doi.org/10.1371/journal.pone.0206514

Crosbie, J., Vachalathiti, R., & Smith, R. (1997). Patterns of spinal motion during walking. *Gait & Posture, 5*(1), 6–12.

D'Amico, M., D'Amico, G., Paniccia, M., Roncoletta, P., & Vallasciani, M. (2010). An integrated procedure for spine and full skeleton multi-sensor biomechanical analysis & averaging in posture gait and cyclic movement tasks. *Studies in Health Technology and Informatics, 158*, 118–126.

D'Amico, M., Kinel, E., D'Amico, G., & Roncoletta, P. (2021, Jun 7). A self-contained 3D biomechanical analysis lab for complete automatic spine and full skeleton assessment of posture, gait and run. *Sensors (Basel), 21*(11). https://doi.org/10.3390/s21113930

Dindorf, C., Konradi, J., Wolf, C., Taetz, B., Bleser, G., Huthwelker, J., … Betz, U. (2020). General method for automated feature extraction and selection and its application for gender classification and biomechanical knowledge discovery of sex differences in spinal posture during stance and gait. *Computer Methods in Biomechanics and Biomedical Engineering, 24*(3), 1–9. https://doi.org/10.1080/10255842.2020.1828375

Dindorf, C., Konradi, J., Wolf, C., Taetz, B., Bleser, G., Huthwelker, J., … Fröhlich, M. (2021a). Classification and automated interpretation of spinal posture data using a pathology-independent classifier and explainable artificial intelligence (XAI). *Sensors, 21*(18). https://doi.org/10.3390/s21186323

Dindorf, C., Konradi, J., Wolf, C., Taetz, B., Bleser, G., Huthwelker, J., … Betz, U. (2021b). Machine learning techniques demonstrating individual movement patterns of the vertebral column: The fingerprint of spinal motion. *Computer Methods in Biomechanics and Biomedical Engineering, 1-11*. https://doi.org/10.1080/10255842.2021.1981884

Drerup, B. (1993). *[The shape of the scoliotic spine. Measurement and mathematical analysis of standard radiographs]. G. Fischer. (Die Form der skoliotischen Wirbelsäule. Vermessung und mathematische Analyse von Standard-Röntgenaufnahmen)*.

Drerup, B. (2014, December 12). Rasterstereographic measurement of scoliotic deformity [journal article]. *Scoliosis, 9*(1), 22. https://doi.org/10.1186/s13013-014-0022-7

Drerup, B., Ellger, B., Meyer Zu Bentrup, F. M., & Hierholzer, E. (2001, Apr). Functional rasterstereographic images. A new method for biomechanical analysis of skeletal geometry. *Orthopade, 30*(4), 242–250. https://doi.org/10.1007/s001320050603 (Rasterstereographische Funktionsaufnahmen. Eine neue Methode zur biomechanischen Analyse der Skelettgeometrie.).

Drerup, B., & Hierholzer, E. (1994, Jan). Back shape measurement using video rasterstereography and three-dimensional reconstruction of spinal shape. *Clinical Biomechanics (Bristol, Avon), 9*(1), 28–36. https://doi.org/10.1016/0268-0033(94)90055-8

Feipel, V., De Mesmaeker, T., Klein, P., & Rooze, M. (2001, Feb). Three-dimensional kinematics of the lumbar spine during treadmill walking at different speeds. *European Spine Journal, 10*(1), 16–22. https://doi.org/10.1007/s005860000199

Gipsman, A., Rauschert, L., Daneshvar, M., & Knott, P. (2014). Evaluating the reproducibility of motion analysis scanning of the spine during walking. *Advances in Medicine, 2014*, Article 721829. https://doi.org/10.1155/2014/721829

Gregersen, G. G., & Lucas, D. B. (1967, Mar). An in vivo study of the axial rotation of the human thoracolumbar spine. *The Journal of Bone and Joint Surgery. American Volume, 49*(2), 247–262. https://www.ncbi.nlm.nih.gov/pubmed/6018729.

Haimerl, M., Nebel, I., Linkerhägner, A., Konradi, J., Wolf, C., Drees, P., & Betz, U. (2022). Comprehensive visualization of spinal motion in gait sequences based on surface topography. *Human Movement Science, 81*. https://doi.org/10.1016/j.humov.2021.102919, 102919. 2022/02/01.

Hierholzer, E. (1993). *Objektive Analyse der Rückenform von Skoliosepatienten*. G. Fischer.

Horst, F., Kramer, F., Schafer, B., Eekhoff, A., Hegen, P., Nigg, B. M., & Schollhorn, W. I. (2016, Sep). Daily changes of individual gait patterns identified by means of support vector machines. *Gait & Posture, 49*, 309–314. https://doi.org/10.1016/j.gaitpost.2016.07.073

Horst, F., Lapuschkin, S., Samek, W., Muller, K. R., & Schollhorn, W. I. (2019, Feb 20). Explaining the unique nature of individual gait patterns with deep learning. *Scientific Reports, 9*(1), 2391. https://doi.org/10.1038/s41598-019-38748-8

Horst, F., Mildner, M., & Schollhorn, W. I. (2017, Oct). One-year persistence of individual gait patterns identified in a follow-up study - a call for individualised diagnose and therapy. *Gait & Posture, 58*, 476–480. https://doi.org/10.1016/j.gaitpost.2017.09.003

Huthwelker, J., Konradi, J., Wolf, C., Westphal, R., Schmidtmann, I., Drees, P., & Betz, U. (2022). Reference Values for 3D Spinal Posture Based on Videorasterstereographic Analyses of Healthy Adults. *Bioengineering, 9*(12), 809. https://doi.org/10.3390/bioengineering9120809

Kakushima, M., Miyamoto, K., & Shimizu, K. (2003, Nov 1). The effect of leg length discrepancy on spinal motion during gait: Three-dimensional analysis in healthy volunteers. *Spine (Phila Pa 1976), 28*(21), 2472–2476. https://doi.org/10.1097/01.Brs.0000090829.82231.4a

Kavanagh, J., Barrett, R., & Morrison, S. (2006, Jul). The role of the neck and trunk in facilitating head stability during walking. *Experimental Brain Research, 172*(4), 454–463. https://doi.org/10.1007/s00221-006-0353-6

Konradi, J. (2022a). *SPSS syntax script to create graphs of spinal motion for a Standardized Gait Cycle*. https://doi.org/10.17632/hbc5fz2xdw.1

Konradi, J. (2022b). *SPSS syntax script to create graphs of spinal motion relative to phases of gait*. https://doi.org/10.17632/5766pxrwh2.1

Konradi, J. (2022c). *Visualizations of rotational curves directly related to gait phases*. https://doi.org/10.17632/j4jwtt82zk.1

Konradi, J. (2022d). *Visualizations of rotational curves within a Standardized Gait Cycle*. https://doi.org/10.17632/m7tbn7vhpf.1

Konz, R. J., Fatone, S., Stine, R. L., Ganju, A., Gard, S. A., & Ondra, S. L. (2006, Nov 15). A kinematic model to assess spinal motion during walking. *Spine (Phila Pa 1976), 31*(24), E898–E906. https://doi.org/10.1097/01.brs.0000245939.97637.ae

Kouwenhoven, J. W., Bartels, L. W., Vincken, K. L., Viergever, M. A., Verbout, A. J., Delhaas, T., & Castelein, R. M. (2007, May 1). The relation between organ anatomy and pre-existent vertebral rotation in the normal spine: Magnetic resonance imaging study in humans with situs inversus totalis. *Spine (Phila Pa 1976), 32*(10), 1123–1128. https://doi.org/10.1097/01.brs.0000261563.75469.b0

Kouwenhoven, J. W., Vincken, K. L., Bartels, L. W., & Castelein, R. M. (2006, Jun 1). Analysis of preexistent vertebral rotation in the normal spine. *Spine (Phila Pa 1976), 31*(13), 1467–1472. https://doi.org/10.1097/01.brs.0000219938.14686.b3

Krott, N. L., Wild, M., & Betsch, M. (2020, Sep). Meta-analysis of the validity and reliability of rasterstereographic measurements of spinal posture. *European Spine Journal, 29*(9), 2392–2401. https://doi.org/10.1007/s00586-020-06402-x

Lamoth, C. J., Beek, P. J., & Meijer, O. G. (2002, Oct). Pelvis-thorax coordination in the transverse plane during gait. *Gait & Posture, 16*(2), 101–114. https://doi.org/10.1016/s0966-6362(01)00146-1

Lamoth, C. J., Meijer, O. G., Wuisman, P. I., van Dieen, J. H., Levin, M. F., & Beek, P. J. (2002, Feb 15). Pelvis-thorax coordination in the transverse plane during walking in persons with nonspecific low back pain. *Spine (Phila Pa 1976), 27*(4), E92–E99.

Leardini, A., Chiari, L., Della Croce, U., & Cappozzo, A. (2005, Feb). Human movement analysis using stereophotogrammetry. Part 3. Soft tissue artifact assessment and compensation. *Gait & Posture, 21*(2), 212–225. https://doi.org/10.1016/j.gaitpost.2004.05.002

Liljenqvist, U., Halm, H., Hierholzer, E., Drerup, B., & Weiland, M. (1998, Jan-Feb). Three-dimensional surface measurement of spinal deformities using video rasterstereography. *Zeitschrift für Orthopädie und Ihre Grenzgebiete, 136*(1), 57–64. https://doi.org/10.1055/s-2008-1044652

MacWilliams, B. A., Rozumalski, A., Swanson, A. N., Wervey, R. A., Dykes, D. C., Novacheck, T. F., & Schwartz, M. H. (2013, Dec 4). Assessment of three-dimensional lumbar spine vertebral motion during gait with use of indwelling bone pins. *The Journal of Bone and Joint Surgery. American Volume, 95*(23), e1841–e1848. https://doi.org/10.2106/JBJS.L.01469

McKay, M. J., Baldwin, J. N., Ferreira, P., Simic, M., Vanicek, N., Wojciechowski, E., … Burns, J. (2017, Oct). Spatiotemporal and plantar pressure patterns of 1000 healthy individuals aged 3-101 years. *Gait & Posture, 58*, 78–87. https://doi.org/10.1016/j.gaitpost.2017.07.004

Michalik, R., Hamm, J., Quack, V., Eschweiler, J., Gatz, M., & Betsch, M. (2020, Sep 8). Dynamic spinal posture and pelvic position analysis using a rasterstereographic device. *Journal of Orthopaedic Surgery and Research, 15*(1), 389. https://doi.org/10.1186/s13018-020-01825-0

Michalik, R., Siebers, H., Classen, T., Gatz, M., Rohof, B., Eschweiler, J., … Betsch, M. (2019, Mar). Comparison of two different designs of forefoot off-loader shoes and their influence on gait and spinal posture. *Gait & Posture, 69*, 202–208. https://doi.org/10.1016/j.gaitpost.2019.02.007

Mohokum, M., Mendoza, S., Udo, W., Sitter, H., Paletta, J. R., & Skwara, A. (2010, Jun 15). Reproducibility of rasterstereography for kyphotic and lordotic angles, trunk length, and trunk inclination: A reliability study. *Spine (Phila Pa 1976), 35*(14), 1353–1358. https://doi.org/10.1097/BRS.0b013e3181cbc157

Mohokum, M., Schülein, S., & Skwara, A. (2015). The validity of Rasterstereography: A systematic review. *Orthopedic Reviews, 7*(3). https://doi.org/10.4081/or.2015.5899, 5899–5899.

Myklebust, M., Magnussen, L., & Inger Strand, L. (2009). Back performance scale scores in people without back pain: Normative data. *Advances in Physiotherapy, 9*(1), 2–9. https://doi.org/10.1080/14038190601090794, 2007/01/01.

Needham, R., Naemi, R., Healy, A., & Chockalingam, N. (2016, Oct). Multi-segment kinematic model to assess three-dimensional movement of the spine and back during gait. *Prosthetics and Orthotics International, 40*(5), 624–635. https://doi.org/10.1177/0309364615579319

Needham, R., Stebbins, J., & Chockalingam, N. (2016). Three-dimensional kinematics of the lumbar spine during gait using marker-based systems: A systematic review. *Journal of Medical Engineering & Technology, 40*(4), 172–185. https://doi.org/10.3109/03091902.2016.1154616

Perry, J., & Burnfield, J. M. (2010). *Gait analysis - Normal and pathological function* (2nd. ed.). SLACK Incorporated.

Póvoa, L. C., Ferreira, A. P. A., Zanier, J. F. C., & Silva, J. G. (2018, Mar). Accuracy of motion palpation flexion-extension test in identifying the seventh cervical spinal process. *Journal of Chiropractic Medicine, 17*(1), 22–29. https://doi.org/10.1016/j.jcm.2017.11.005

Raspe, H. (2012). *Rückenschmerzen 53*. Gesundheitsberichterstattung des Bundes.

Schmidtmann, I., & Konradi, J. (2022). *SAS syntax script for merging export files*. https://doi.org/10.17632/mtd5x49mkc.1

Schöllhorn, W. I., Nigg, B. M., Stefanyshyn, D. J., & Liu, W. (2002, Apr). Identification of individual walking patterns using time discrete and time continuous data sets. *Gait & Posture, 15*(2), 180–186. https://doi.org/10.1016/s0966-6362(01)00193-x

Schubert, P., & Kirchner, M. (2014). Ellipse area calculations and their applicability in posturography. *Gait & Posture, 39*(1), 518–522. https://doi.org/10.1016/j.gaitpost.2013.09.001, 2014/01/01.

Schulte, T. L., Hierholzer, E., Boerke, A., Lerner, T., Liljenqvist, U., Bullmann, V., & Hackenberg, L. (2008, Feb). Raster stereography versus radiography in the long-term follow-up of idiopathic scoliosis. *Journal of Spinal Disorders & Techniques, 21*(1), 23–28. https://doi.org/10.1097/BSD.0b013e318057529b

Semaan, M. B., Wallard, L., Ruiz, V., Gillet, C., Leteneur, S., & Simoneau-Buessinger, E. (2022, Feb). Is treadmill walking biomechanically comparable to overground walking? A systematic review. *Gait & Posture, 92*, 249–257. https://doi.org/10.1016/j.gaitpost.2021.11.009

Suppé, B. (2014). In I. Spirgi-Gantert, & B. Suppé (Eds.), *FBL Klein-Vogelbach functional kinetics – Die Grundlagen* (7th ed.). Springer-Verlag.

Suppé, B., & Bongarz, M., & (Eds.).. (2013). *FBL Klein-Vogelbach Functional Kinetics praktisch angewandt. Gehen - Analyse und Intervention*. Springer. https://doi.org/10.1007/978-3-642-22076-0

Troendle, J. F., & Yu, K. F. (2003). Estimation of sample size for reference interval studies. *Biometrical Journal, 45*(5), 561–572.

Turner-Smith, A. R. (1988). A television/computer three-dimensional surface shape measurement system. *Journal of Biomechanics, 21*(6), 515–529. https://doi.org/10.1016/0021-9290(88)90244-8

Turner-Smith, A. R., Harris, J. D., Houghton, G. R., & Jefferson, R. J. (1988). A method for analysis of back shape in scoliosis. *Journal of Biomechanics, 21*(6), 497–509. https://doi.org/10.1016/0021-9290(88)90242-4

Vogt, L., Pfeifer, K., Portscher, & Banzer, W. (2001, Sep 1). Influences of nonspecific low back pain on three-dimensional lumbar spine kinematics in locomotion. *Spine (Phila Pa 1976), 26*(17), 1910–1919. https://doi.org/10.1097/00007632-200109010-00019

Westphal, R., & Konradi, J. (2022). *SAS syntax script for creation of a Standardized Gait Cycle*. https://doi.org/10.17632/k29mpr863y.1

Wolf, C., Betz, U., Huthwelker, J., Konradi, J., Westphal, R. S., Cerpa, M., … Drees, P. (2021, Dec 4). Evaluation of 3D vertebral and pelvic position by surface topography in asymptomatic females: Presentation of normative reference data. *Journal of Orthopaedic Surgery and Research, 16*(1), 703. https://doi.org/10.1186/s13018-021-02843-2